Korean J. Chem. Eng., **21**(6), 1126-1138 (2004)

Flow Directions in Gas Assisted Injection Molding When Cavities of Square Flat Plates and Pipes are Involved 2. Development of Time-dependent Flow Model

Kwang-Hee Lim† and Soo-Hyeun Hong

Department of Chemical Engineering, Daegu University, Kyungsan, Kyungbook 712-714, Korea
(*Received 2 May 2004 • accepted 7 August 2004*)

Abstract–For such conditions that $(H/R_0)^2$ is replaced by ε (that is the order of 10^{-1}) and $\hat{\theta}^2$ is the order of one, the rule of thumb for an approximated flow model was introduced in part 1 of the paper to show, in qualitative way, whether the resistance of the relatively thick cavity of two square plates might affect the gas direction in GAIM under the afore-said geometry. Subsequently, various simulations were performed by using Moldflow (version of MPI 4.0) under the conditions that all dimensions of cavity of two square plates and pipes were fixed except for the diameters of pipes, and the results of simulation were compared with the results of a rule of thumb (RT1) containing the approximated flow model as well as those of another rule of thumb (RT2) without the resistance of the relatively thick cavity of two square plates. There were some exceptional cases where RT1 or RT2 were not consistent with the simulation results (i.e., flow directions). Thus such a developed model as time-dependent model was required to describe transient behavior of the interface between gas phase and resin phase instead of comparison of initial velocities in upper side and lower side of the configuration, which was proposed and utilized to compare with the results of Moldflow in this 2nd part of the paper. The predictions of the developed flow model were so quite consistent with the results of simulation that the proposed time-dependent flow model may be referred to describe very well the transient behavior of the movement of the interface of gas and melt-resin in the cavities. In addition, a timedependent model was also established and was used to compare with the results of Moldflow when cavities of pipes and runners were involved in configuration. It is amazing that the proposed developed model was able to predict exactly the cross-over between the trajectories of interface of upper and lower side, and it is also surprising to describe the time dependent behavior so well that the result of the predictions by the developed model were quite consistent to the results of simulation by Moldflow.

Key words: Gas Assisted Injection Molding, Rule of Thumb, Preferred Direction of Gas, The Least Resistance to Initial-resin Velocity

INTRODUCTION

The rule of thumb on the direction of gas flow for GAIM has been investigated [Lim and Soh, 1999; Soh, 2000; Soh and Lim, 2002; Lim and Lee, 2003; Lim, 2004a, b, c; Lim and Hong, 2004], and simulation packages were used to verify the gas direction predicted by the rule of thumb. For such conditions that $(H/R_0)^2$ is replaced by ε (that is the order of 10^{-1}) and $\hat{\theta}^2$ is the order of one, the rule of thumb for an approximated flow model was introduced in part 1 of the paper [Lim, 2004c] to show, in qualitative way, whether the resistance of the relatively thick cavity of two square plates may affect the gas direction in GAIM under the afore-said geometry. Subsequently various simulations were performed using Moldflow (version of MPI 4.0) under the conditions that all dimensions of cavity of two square plates and pipes were fixed except for the diameters of pipes and the results of simulation were compared with the results of rule of thumb (RT1) containing the approximated flow model as well as those of another rule of thumb (RT2) without the resistance of the relatively thick cavity of two square plates. There were some exceptional cases where RT1 or RT2 were not consistent with the simulation results (i.e., flow directions). Thus such a developed model as time-dependent model is required to describe transient behavior of the interface between gas phase and resin phase instead of comparison of initial velocities in upper side and lower side of the configuration, which shall be proposed and utilized to compare with the results of Moldflow in this 2nd part of the paper. In addition, a timedependent model shall be also established and used to compare with the results of Moldflow when cavities of pipes and runners were involved in the configuration.

†To whom correspondence should be addressed.
E-mail: khlim@daegu.ac.kr

METHODS

1. Theory

1-1. Flow Model through Pipes

The flow of a Newtonian fluid in pipes may be described by the famous Hagen-Poiseuille law as:

$$\Delta P = \frac{32\mu L V}{D^2} \tag{1}$$

Under the proposed geometry (Figs. 1 and 2) the length of resin in runners or pipes (initially full of resin) decreases at the same rate as the velocity of gas penetration unlike the length of moving resin in a cylindrical geometry of which the decreasing rate is mainly attributed to the accumulation of coated layer on its surface of mold. One may replace the average velocity of fluid (V) with dL/dt where L is the decreasing length of resin. Then, assuming that Eq. (1) may be in the condition of quasi-steady state and neglecting coated layer

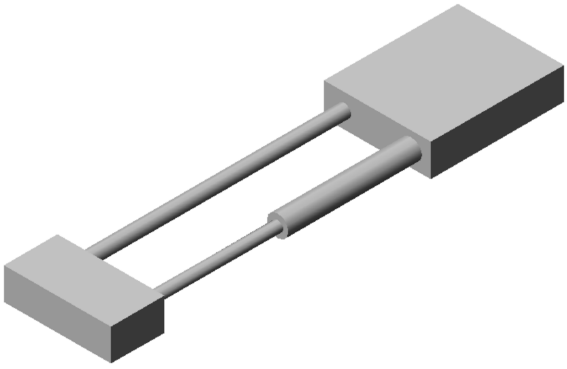

Fig. 1. A cavity composed of two pipes, pipe 1 and pipe 2, connected in parallel. Thick cavities of two square flat plates (SFP) are attached to each side of these pipes. The length, depth and width of a cavity between two SFP were 20 mm, 12 mm and 40 mm, respectively.

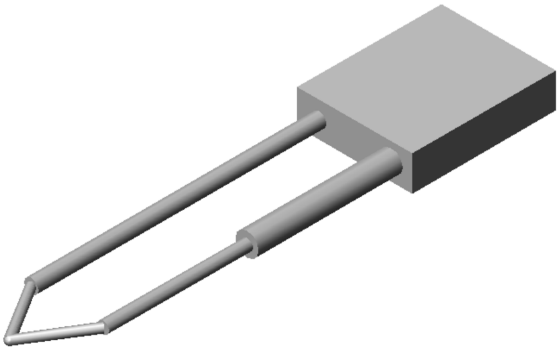

Fig. 2. A cavity composed of two pipes, pipe 1 and pipe 2, connected in parallel. At the left side of these pipes branching runners are replaced for a thick cavity of two square plates to deliver resin to both sides of pipes.
*"Unpenetrated length" in Fig. 3-19 denotes the value deducted by gas penetration length from total geometrical length (i.e., length between gas injection point and connection of two SFP with a pipe, plus total pipe length).

on the surface of molds, the length of resin (L) may be described as:

$$L^2(0)-L^2(t)=\frac{\Delta P D^2 t}{16\mu} \tag{2}$$

1-2. Flow Model under the Cavity between Two Square Flat Plates

The expression of the flow rate of a Newtonian fluid of Eq. (7) assumed in the condition of quasi-steady state was obtained as the flow model for the fan shaped geometry in GAIM [Lim, 1999, 2004a].

$$Q=\hat{\theta}rH\langle v_r\rangle=2\int_0^h v_r(r,z)\hat{\theta}r\,dz=\frac{2\hat{\theta}h^3}{3}\frac{P_1-P_0}{\mu\ln\frac{R_0}{R_1}} \tag{3}$$

if $\rho\bar{v}_r H/\mu(H/R_0)\ll 1$, $(H/R_0)^2 1/\hat{\theta}^2\ll 1$ and $(H/R_0)^2\ll 1$

When $\rho\bar{v}_r H/\mu(H/R_0)\ll 1$, and $(H/R_0)^2 1/\hat{\theta}^2$ and $(H/R_0)^2$ are the orders of 10^{-1}, the expression of the flow rate of a Newtonian fluid under fan-shaped geometry may be also approximated as Eq. (3) [Lim , 2004c].

Then pressure drop between R_1 and R_0 may be written in terms of flow rate as below.

$$\Delta P=\frac{12\mu Q}{H^3\hat{\theta}}\ln\frac{R_0}{R_1}=Q\frac{12\mu}{H^3\hat{\theta}}\ln\frac{R_0}{R_1} \tag{4}$$

Using the relation of $Q=R_1\hat{\theta}HV_1$, the flow rate may be expressed in such a way as:

$$Q=\frac{\hat{\theta}}{2}H\frac{dR_1^2}{dt} \tag{5}$$

One may substitute Eq. (5) into Eq. (4) assumed in the condition of quasi-steady state and may separate variables in both sides, after which both sides are integrated to develop the flow model to show dynamics of R_1 and R_0 as below.

$$\therefore\int_0^t \Delta P\,dt=\frac{6\mu}{H^2}\int_{R_1^2(0)}^{R_1^2}\ln\frac{R_0}{R_1}dR_1^2 \tag{6}$$

where $R_0(0)$ and $R_1(0)$ are the radius of polymer shut-off and the radius of gas nozzle, respectively.

Under the proposed geometry R_0 is fixed so that the volume of melt polymer in the cavity between two square flat plates (SFP) may not be conserved but decrease due to leaking through pipes attached to the cavity between two SFP. Thus time-evolution of radius of the interface between gas and melt-polymer (i.e., $R_1(t)$) may be implicitly expressed as below, neglecting the coated layer on the surface of molds.

$$\begin{aligned}\Delta P t=&\frac{6\mu}{H^2}\ln R_0(R_1^2(t)-R_1^2(0))\\&-\frac{3\mu}{H^2}\{R_1^2(t)\ln R_1^2(t)-R_1^2(0)\ln R_1^2(0)-(R_1^2(t)-R_1^2(0))\}\end{aligned} \tag{7}$$

1-3. Flow Model When Cavities of Pipes and Thick Plates are Involved in Configuration

Since pipes are located in serial and parallel position as in Fig. 1, the section of pipes may be divided into upper part and lower part of the proposed geometry. When the combined geometry of pipes and a cavity between two SFP is considered as in Fig. 1, the model-predictions of gas penetration length may be categorized in two regions, i.e., the cavity between two SFP and the pipe. Then one may consider the case where a gas leading front (i..e, the interface between gas and melt resin) exists in the region of the cavity between two SFP, as well as the case where a gas leading front exists in the region of a pipe.

1-3-1. Gas Penetration in the Upper Part

The vertex angle of a triangle ($\hat{\theta}$) is formed in accordance with the shape of gas penetration in the cavity between two SFP and the half of $\hat{\theta}$ was assigned as a vertex angle for the upper part of fan-shaped gas penetration in the cavity between two SFP in order to consider the volumetric flow rate of gas through an upper pipe.

For the former case ($0\le t\le\Delta t$) the length of gas penetration may be evluated as below.

$$\begin{aligned}\Delta P t=&\frac{6\mu}{H^2}\ln R_0(R_1^2(t)-R_1^2(0))\\&-\frac{3\mu}{H^2}\{R_1^2(t)\ln R_1^2(t)-R_1^2(0)\ln R_1^2(0)-(R_1^2(t)-R_1^2(0))\}\\&+\hat{\theta}H\frac{32\mu}{\pi}\frac{L_1(0)}{D_1^4}(R_1^2(t)-R_1^2(0))\end{aligned} \tag{8}$$

for $t<\Delta t$:

$$\Delta t=\left[\frac{6\mu}{H^2}\ln R_0(R_0^2-R_1^2(0))-\frac{3\mu}{H^2}\{R_0^2\ln R_0^2-R_1^2(0)\ln R_1^2(0)-(R_0^2-R_1^2(0))\}+\hat{\theta}H\frac{32\mu}{\pi}\frac{L_1(0)}{D_1^4}(R_0^2-R_1^2(0))\right]/(\Delta P) \quad (9)$$

For the latter case ($t\geq\Delta t$) the time-dependent length of remaining resin in the upper pipe may be described as below.

$$\left[\frac{L_1^2(0)-L_1(t)^2}{D_1^2}\right]=\frac{\Delta P}{16\mu}(t-\Delta t) \quad (10)$$

1-3-2. Gas Penetration in the Lower Part

Like the upper part, the half of $\hat{\theta}$ was assigned as a vertex angle for the lower part of fan-shaped gas penetration in the cavity between two SFP in order to consider the volumetric flow rate of gas through a upper pipe.

For the former case the length of gas penetration may be evluated as below.

$$\Delta Pt=\frac{6\mu}{H^2}\ln R_0(R_1'^2(t)-R_1^2(0))-\frac{3\mu}{H^2}\{R_1'^2(t)\ln R_1'^2(t)-R_1^2(0)\ln R_1^2(0)-(R_1'^2(t)-R_1^2(0))\}+\hat{\theta}H\frac{32\mu}{\pi}\left(\frac{L_{21}(0)}{D_{21}^4}+\frac{L_{22}(0)}{D_{22}^4}\right)(R_1'^2(t)-R_1^2(0)) \quad (11)$$

for $t<\Delta t$:

$$\Delta t=\left[\frac{6\mu}{H^2}\ln R_0(R_0^2-R_1^2(0))-\frac{3\mu}{H^2}\{R_0^2\ln R_0^2-R_1^2(0)\ln R_1^2(0)-(R_0^2-R_1^2(0))\}+\hat{\theta}H\frac{32\mu}{\pi}\left(\frac{L_{21}(0)}{D_{21}^4}+\frac{L_{22}(0)}{D_{22}^4}\right)(R_0^2-R_1^2(0))\right]/(\Delta P) \quad (12)$$

where the prime (′) denotes the lower side of fan-shaped gas penetration in the cavity between two SFP.

For the latter case the time-dependent length of remaining resin in the lower pipe may be described as below.

(1) When a gas-leading front exists in $pipe_{21}$ the length of remaining resin in a pipe becomes the sum of $L_{21}(t)$ and $L_{22}(0)$. The dynamic behavior of $L_{21}(t)$ may be expressed as;

$$\frac{L_{21}^2(0)-L_{21}^2(t)}{2D_{21}^2}+\frac{L_{22}(0)D_{21}^2(L_{21}(0)-L_{21}(t))}{D_{22}^4}=\frac{\Delta P}{32\mu}(t-\Delta t) \quad (13)$$

for $\Delta t<t<\Delta t+\Delta t_1$

$$\text{where } \frac{L_{21}^2(0)}{2D_{21}^2}+\frac{L_{22}(0)D_{21}^2L_{21}(0)}{D_{22}^4}=\frac{\Delta P}{32\mu}\Delta t_1 \quad (14)$$

(2) When a gas-leading front exists in $pipe_{22}$ the dynamic behavior of $L_{22}(t)$ becomes:

$$\frac{L_{22}^2(0)-L_{22}^2(t)}{D_{22}^4}=\frac{\Delta P}{16\mu}(t-\Delta t-\Delta t_1) \quad (15)$$

for $t>\Delta t+\Delta t_1$

1-4. Flow Model When Cavities of Pipes and Runners are Involved in Configuration

Since pipes and runners are located in serial and parallel position as in Fig. 2, they may be divided into upper part and lower part of the proposed geometry. When the combined geometry of pipes and a runner is considered as in Fig. 2, the model-predictions of gas penetration length may be categorized in two regions, i.e., the runner and the pipe. Then one may consider the case that a gas leading front (i.e., the interface between gas and melt resin) exists in the region of a runner as well as the case that a gas leading front exists in the region of a pipe.

1-4-1. Gas Penetration in the Upper Part

For the former case ($0\leq t\leq\Delta t'$) the length of gas penetration may be evluated as below.

$$\left[\frac{1}{8D_1'^2}(L_1'^2(0)-L_1'^2(t))+\frac{L_1(0)}{4}\frac{D_1'^2}{D_1^4}(L_1'(0)-L_1'(t))\right]=\frac{\Delta P}{128\mu}t \quad (16)$$

where remaining total length filled with resin becomes $L_1'(t)+L_1(0)$.

for $0<t<\Delta t'$:

$$\Delta t'=\frac{\left[\frac{L_1'(0)^2}{2D_1'^2}+\frac{L_1(0)L_1'(0)D_1'^2}{D_1^4}\right]}{\frac{\Delta P}{32\mu}} \quad (17)$$

For the latter case ($t\geq\Delta t'$) the time-dependent length of remaining resin in the lower pipe may be described as below.

$$\frac{1}{8D_1^2}(L_1^2(0)-L_1^2(t-\Delta t'))=\frac{\Delta P}{128\mu}(t-\Delta t') \quad (18)$$

1-4-2. Gas Penetration in the Lower Part

For the former case ($0\leq t\leq\Delta t'$) the length of gas penetration may be evluated as below.

$$\left[\frac{1}{8D_1'^2}(L_1'^2(0)-L_1'^2(t))+\frac{L_2(0)}{4}D_2'^2\left(\frac{1}{D_{21}^4}+\frac{1}{D_{22}^4}\right)(L_2'(0)-L_2'(t))\right]=\frac{\Delta P}{128\mu}t \quad (19)$$

where remaining total length filled with resin becomes $L_1'(t)+L_{21}(0)+L_{22}(0)$.

for $0<t<\Delta t'$:

$$\Delta t'=\frac{\left[\frac{L_2'^2(0)}{2D_2'^2}+\frac{L_2(0)L_2'(0)D_2'^2}{\frac{1}{D_{11}^4}+\frac{1}{D_{22}^4}}\right]}{\frac{\Delta P}{32\mu}} \quad (20)$$

For the latter case ($\Delta t'\leq t\leq\Delta t'+t_1$) the time-dependent length of remaining resin in the lower first pipe may be described as below.

$$\left[\frac{1}{8D_{21}^2}(L_{21}^2(0)-L_{21}^2(t_1))+\frac{L_{22}(0)}{4}\frac{D_{21}^2}{D_{22}^4}(L_{21}(0)-L_{21}(t_1))\right]=\frac{\Delta P}{128_\mu}t_1 \quad (21)$$

where $t_1=t-\Delta t'$

For another latter case ($\Delta t'+\Delta t_1\leq t\leq\Delta t'+\Delta t_1+t_2$) the time-dependent length of remaining resin in the lower second pipe may be described as below.

$$\left[\frac{1}{8D_{22}^2}(L_{22}^2(0)-L_{22}^2(t_2))\right]=\frac{\Delta P}{128\mu}t_2 \quad (22)$$

for $t_2=t-\Delta t'-\Delta t_1'$:

$$\Delta t_1'=\frac{\left[\frac{L_{21}^2(0)}{2D_{21}^2}+\frac{L_{22}(0)L_{21}(0)D_{21}^2}{D_{22}^4}\right]}{\frac{\Delta P}{32\mu}} \quad (23)$$

2. Simulations and Model-predictions

The simulation and model-prediction were performed under the geometry composed of two pipes (pipe 1 and pipe 2) connected in parallel as well as two relatively thick cavities between two SFP attached to each side of them as shown in Fig. 1. The initial polymer shut-off totally filled the cavities of a pipe 1 and pipe 2 (center) as well as the left (polymer/gas nozzle side) cavity between two square-flat plates (SFP). On the other hand, the right cavity between two SFP was partially filled by 85-90% with melt resin due to a short shot. The length, depth and width of a cavity between two SFP were 20 mm, 12 mm and 40 mm, respectively. Pipe 1 and pipe 2 were composed of two identical or different pipes, respectively, each of which was 50 mm long. Both ends of pipe 1 and pipe 2 were connected to the left and right cavities between two SFP, respectively. The connection points between pipes and the cavities between two SFP were located at the centers of the 1st and 2nd half of the cavity-width. Thus the vertex angle ($\hat{\theta}$) of fan-shaped cavity was initially π and it remained at this value at the incipient stage of gas penetration. However, the vertex angle ($\hat{\theta}$) became smaller when the interface between gas and resin existed in the cavity between two SFP, and it reached the value of 0.93 radian of a triangle formed connecting a gas nozzle and two junctions between SFP and pipes when the interface between gas and melt resin approached the junctions between SFP and pipes. The value of the vertex angle ($\hat{\theta}$) was chosen as $2/3\pi$, on average, as control to apply to the proposed flow model. The values of the vertex angle ($\hat{\theta}$) were also adopted, 0.93 and π, as reference-vertex angles. In addition, simulation and model-prediction were performed under the geometry composed of two pipes (pipe 1 and pipe 2) connected in parallel as well as a runner and a relatively thick cavity attached to L. H. S. and R. H. S. of them, respectively, as shown in Fig. 2. The simulation conditions were as the same as given in Table 1 when the commercial software of MOLDFLOW (version of MPI 4.1) was used to perform the simulations of the cases as shown in Tables 2 and 3.

Tables 2 and 3 show geometrical conditions situated when the cavities of pipes (center) as well as two cavities between two SFP (left and right) and the cavities of pipes (center), a runner as well as a cavity between two SFP (right) were involved in the configuration as in Fig. 1 and Fig. 2, respectively. The diameter of each pipe varied from 2 mm to 10 mm as in Tables 2 and 3. For each case of Tables 2 and 3 the volume ratio of resin filling at polymer shut-off was chosen between 85%-95% to avoid blow-through at the stage of gas injection. Finite element method (FEM) was adopted to simulate the center (a pipe) and the left and right hand sides (SFP), modeled with line-elements and triangle-elements respectively, of Fig. 1 in the environment of MOLDFLOW (version of MPI 4.1). In a similar manner, as in Fig. 2, finite element method (FEM) was adopted to simulate the center (a pipe), the left (runner) and the right hand side (SFP), modeled with line-elements, line elements and triangle-elements, respectively.

Table 1. Simulation conditions of MOLDFLOW

Simulation factor	Description
Resin filling	Short shot molding (85-95%)
Gas control	Volume control
Resin	PET(DP400)
Resin melt temperature	210 °C
Mold temperature	100 °C
Gas injection pressure	15 M pascal
Gas delay time	0.5 sec
Gas piston time	1 sec

Table 2. Various geometrical conditions of pipes as in Fig. 1

Case	D_1	D_{21}	D_{22}
Fig. 3(a)	5 mm	6 mm	4 mm
Fig. 4(a)	5 mm	8 mm	4 mm
Fig. 5(a)	5 mm	10 mm	4 mm
Fig. 6(a)	5 mm	2 mm	8 mm
Fig. 7(a)	5 mm	4 mm	8 mm
Fig. 8(a)	5 mm	5 mm	4.5 mm
Fig. 9(a)	4.5 mm	5 mm	4.5 mm
Fig. 10(a)	4.5 mm	7.5 mm	5 mm
Fig. 11(a)	6 mm	5.5 mm	6 mm

Table 3. Various geometrical conditions of runners and pipes as in Fig. 2

Case	D_1'	D_2'	D_1	D_{21}	D_{22}
Fig. 12(a)	3 mm	3 mm	5 mm	8 mm	4 mm
Fig. 13(a)	3 mm	3 mm	5 mm	10 mm	4 mm
Fig. 14(a)	3 mm	3 mm	5 mm	2 mm	8 mm
Fig. 15(a)	3 mm	3 mm	5 mm	4 mm	8 mm
Fig. 16(a)	3 mm	3 mm	5 mm	4.2 mm	8 mm
Fig. 17(a)	3 mm	3 mm	5 mm	7 mm	4.5 mm
Fig. 18(a)	3 mm	3 mm	5 mm	8 mm	4.5 mm
Fig. 19(a)	3 mm	3 mm	5 mm	9 mm	4.5 mm

RESULTS AND DISCUSSION

1. Situation when Cavities of Pipes and Thick Plates are Involved in Configuration

Table 4 shows the predicted directions of gas flow of time-dependent developed flow model (Figs. 3(c) through 3(e) to 11(c) through 11(e)) as well as the results of simulation of Moldflow (Figs. 3(a)-(b) to 11(a)-(b)). Each length of gas penetration to both directions of Figs. 3(a) to 11(a) is shown as in Figs. 3(b) to 11(b), respectively. The predictions of developed flow model were so quite consistent to the results of simulation that the proposed time-dependent flow model may be referred to describe very well the transient behavior of the movement of the interface of gas and melt-resin in the cavities. As in Table 4, the result of simulation of Fig. 7(a) (i.e., U→L) may be interpreted such that the gas flow was faster at the upper side of the cavity of SFP and the direction of gas flow was finally reversed to the lower side of the geometry when the interface of

Table 4. Flow directions of simulation and developed flow model in Fig. 1

Case (a-b)	Simulation-results	Model-prediction (c-e)	Predicted gas-direction		
			$\hat{\theta}$: 0.93 (c)	$2/3\pi$(d)	π(e)
Fig. 3(a)-(b)	U	Fig. 3(c)-(e)	U	U	U
Fig. 4(a)-(b)	U	Fig. 4(c)-(e)	U	U	U
Fig. 5(a)-(b)	U	Fig. 5(c)-(e)	U	U	U
Fig. 6(a)-(b)	U	Fig. 6(c)-(e)	U	U	U
Fig. 7(a)-(b)	U→L	Fig. 7(c)-(e)	U→L	U	U
Fig. 8(a)-(b)	U	Fig. 8(c)-(e)	U	U	U
Fig. 9(a)-(b)	L	Fig. 9(c)-(e)	L	L	L
Fig. 10(a)-(b)	L	Fig. 10(c)-(e)	L	L	L
Fig. 11(a)-(b)	U	Fig. 11(c)-(e)	U	U	U

*"U" and "L" denote "Upper" and "Lower", respectively.
*"U→L" denotes that gas flow is faster at the cavity of SFP of upper side but its direction finally turns to lower side of the geometry.

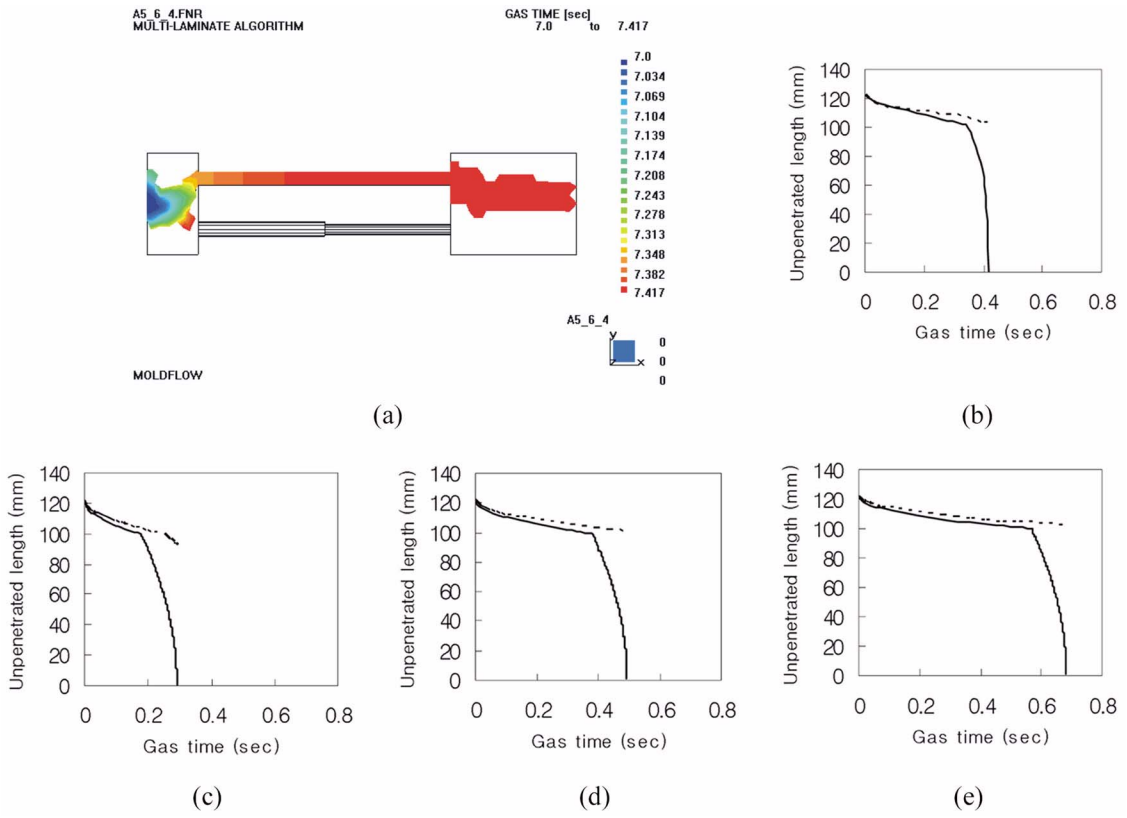

Fig. 3. (a) Pipe 11 with a diameter of 5 mm and a length of 50 mm is connected to pipe 12 with a diameter of 5 mm and a length of 50 mm. Pipe 21 with a diameter of 6 mm and a length of 50 mm is connected in series with pipe 22 with a diameter of 4 mm and a length of 50 mm; (b) Time evolution of gas penetration length from Fig. 3(a); Model predictions; (c) $\hat{\theta}$=0.93; (d) $\hat{\theta}$=2/3π; (e) $\hat{\theta}$=π (solid line: upper side, dotted line: lower side).

gas and melt-resin was passing through the cavity of pipes. This is consistent with the results of part 1 of the paper where RT1 was greater than unity while RT2 was less than unity. Furthermore, the effect of RT2 was possibly expected as greater than that of RT1 in the result of simulation of Fig. 7(a) that the directiuon of gas flow would be finally changed to the lower side of the cavity in the geometry. However, there was no idea which one finally prevails in part 1 of the paper, while the proposed developed model is able to provide the idea and to describe the time-dependent behavior of the interface of gas and melt-resin. On the other hand, the predicted gas-flow direction of time dependent developed flow model was more appropriate, as in Fig. 7(c) to (e), when the value of $\hat{\theta}$ was applied as 0.93 radian than when those was applied as $2/3\pi$ or π. This may be interpreted as that the effect of RT1 became less due to decreased difference of resistances, since the difference of the flow rates between upper side and lower side of the geometry was reduced when the value of $\hat{\theta}$ became less, while the effect of RT2 had nothing to do with the value of $\hat{\theta}$. However in other cases the

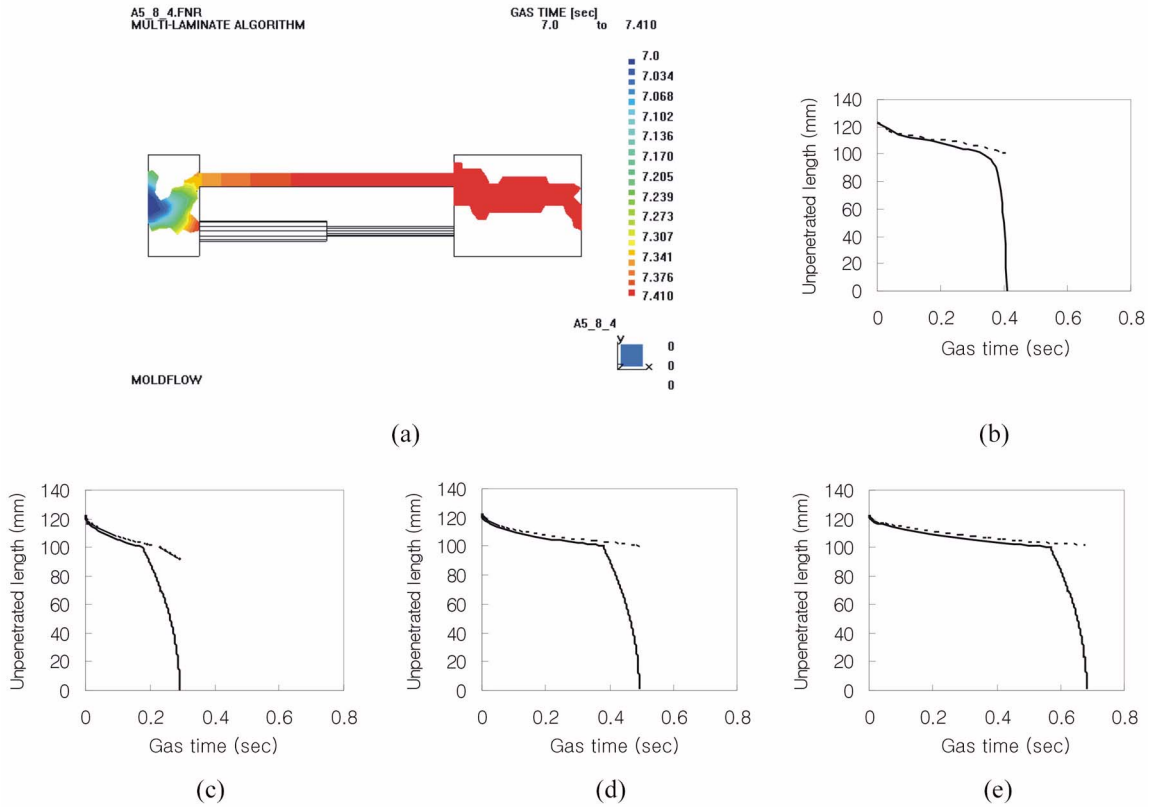

Fig. 4. (a) The geometry is the same as Fig. 3 except that diameter of pipe 21 is 8 mm; (b) Time evolution of gas penetration length from Fig. 4(a); Model predictions; (c) $\hat{\theta}$=0.93; (d) $\hat{\theta}$=2/3π; (e) $\hat{\theta}$=π (solid line: upper side, dotted line: lower side).

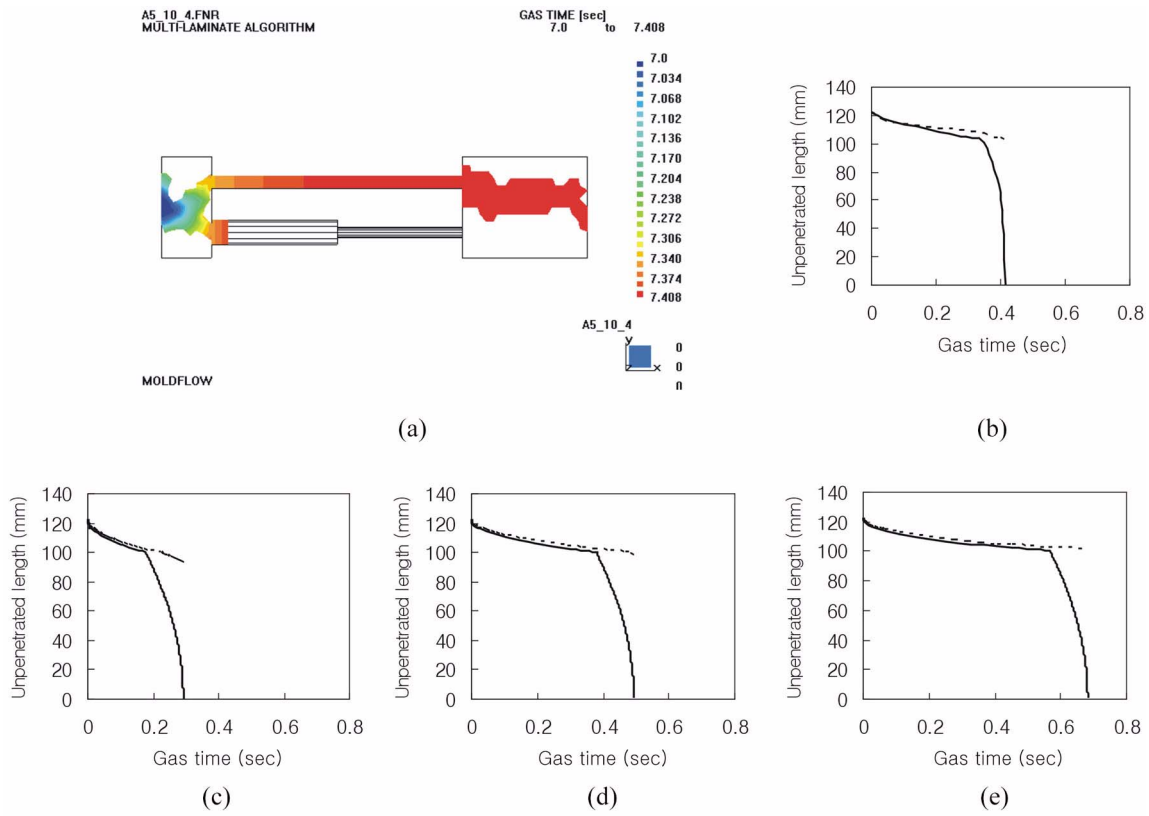

Fig. 5. (a) The geometry is the same as Fig. 3 except that diameter of pipe 21 is 10 mm; (b) Time evolution of gas penetration length from Fig. 5(a); Model predictions; (c) $\hat{\theta}$=0.93; (d) $\hat{\theta}$=2/3π; (e) θ=π (solid line: upper side, dotted line: lower side).

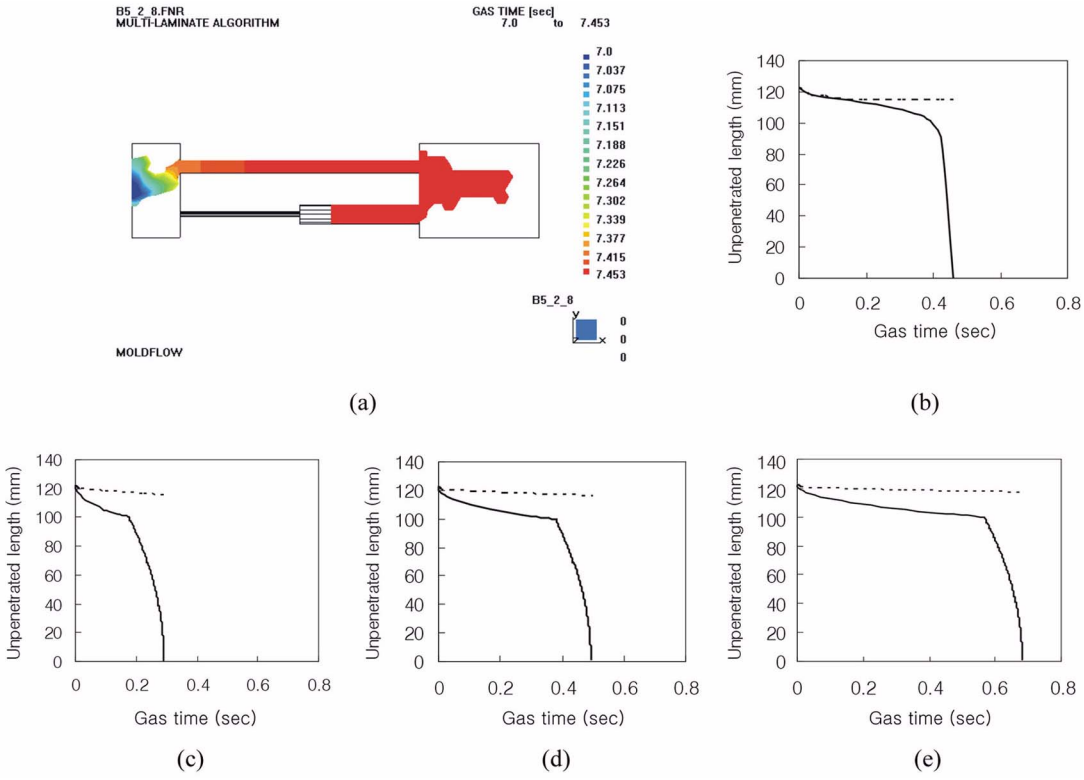

Fig. 6. (a) Pipe 11 with a diameter of 5 mm and a length of 50 mm is connected to pipe 12 with a diameter of 5 mm and a length of 50 mm. Pipe 21 with a diameter of 2 mm and a length of 50 mm is connected in series with pipe 22 with a diameter of 8 mm and a length of 50 mm; (b) Time evolution of gas penetration length from Fig. 6(a); Model predictions; (c) $\hat{\theta}$=0.93; (d) $\hat{\theta}$=2/3π; (e) $\hat{\theta}$=π (solid line: upper side, dotted line: lower side).

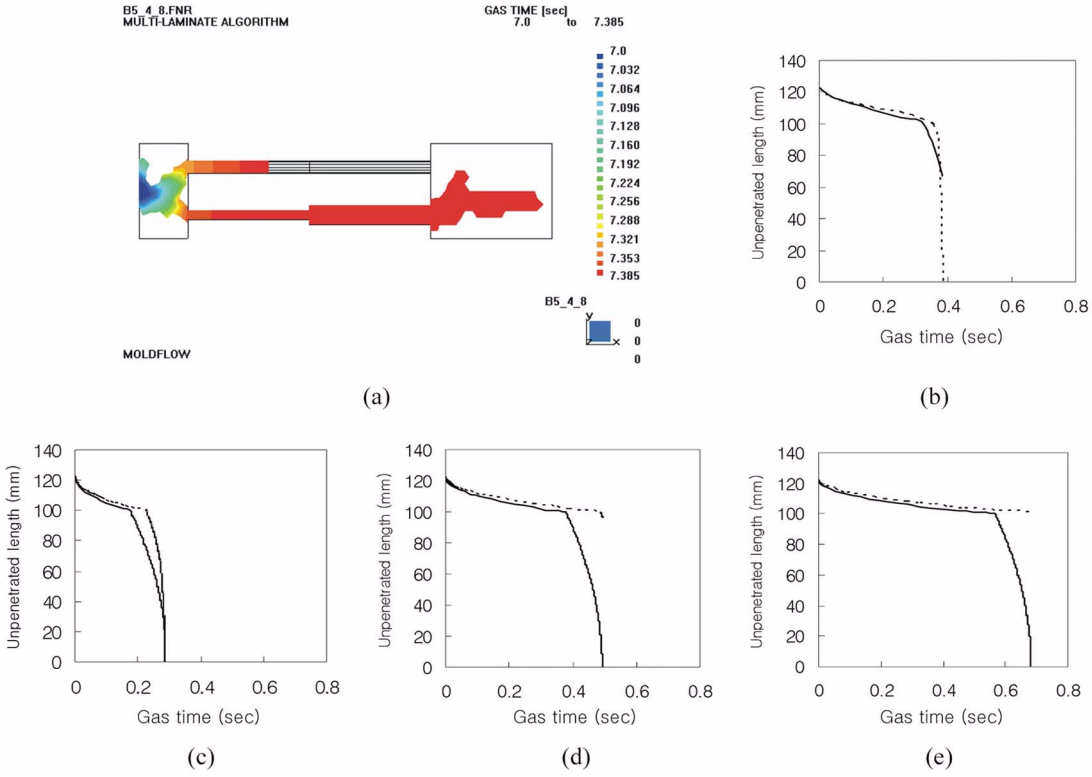

Fig. 7. (a) The geometry is the same as Fig. 6 except that diameter of pipe 21 is 4 mm; (b) Time evolution of gas penetration length from Fig. 7(a); Model predictions; (c) $\hat{\theta}$=0.93; (d) $\hat{\theta}$=2/3π; (d) $\hat{\theta}$=π (solid line: upper side, dotted line: lower side).

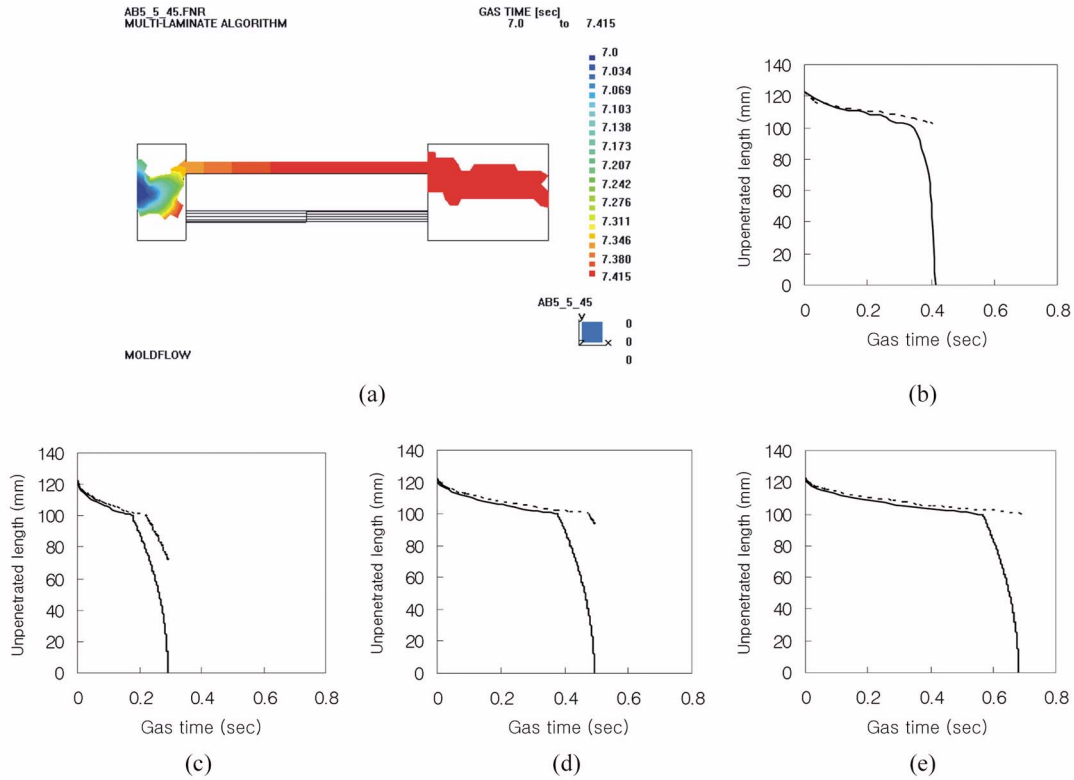

Fig. 8. (a) Pipe 11 with a diameter of 5 mm and a length of 50 mm is connected to pipe 12 with a diameter of 5 mm and a length of 50 mm. Pipe 21 with a diameter of 5 mm and a length of 50 mm is connected in series with pipe 22 with a diameter of 4.5 mm and a length of 50 mm; (b) Time evolution of gas penetration length from Fig. 8(a); Model predictions; (c) $\hat{\theta}$=0.93; (d) $\hat{\theta}$=2/3π; (e) $\hat{\theta}$=π (solid line: upper side, dotted line: lower side).

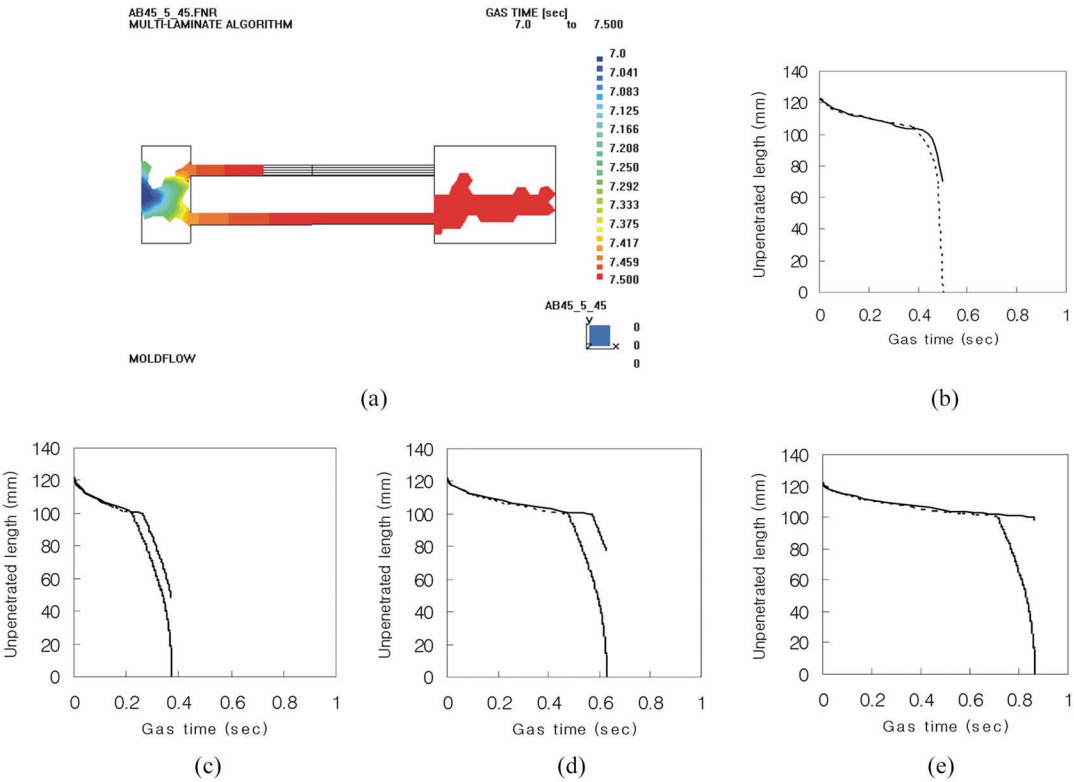

Fig. 9. (a) The geometry is the same as Fig. 8 except that diameter of pipe 1 is 4.5 mm; (b) Time evolution of gas penetration length from Fig. 9(a); Model predictions; (c) $\hat{\theta}$=0.93; (d) $\hat{\theta}$=2/3π; (e) $\hat{\theta}$=π (solid line: upper side, dotted line: lower side).

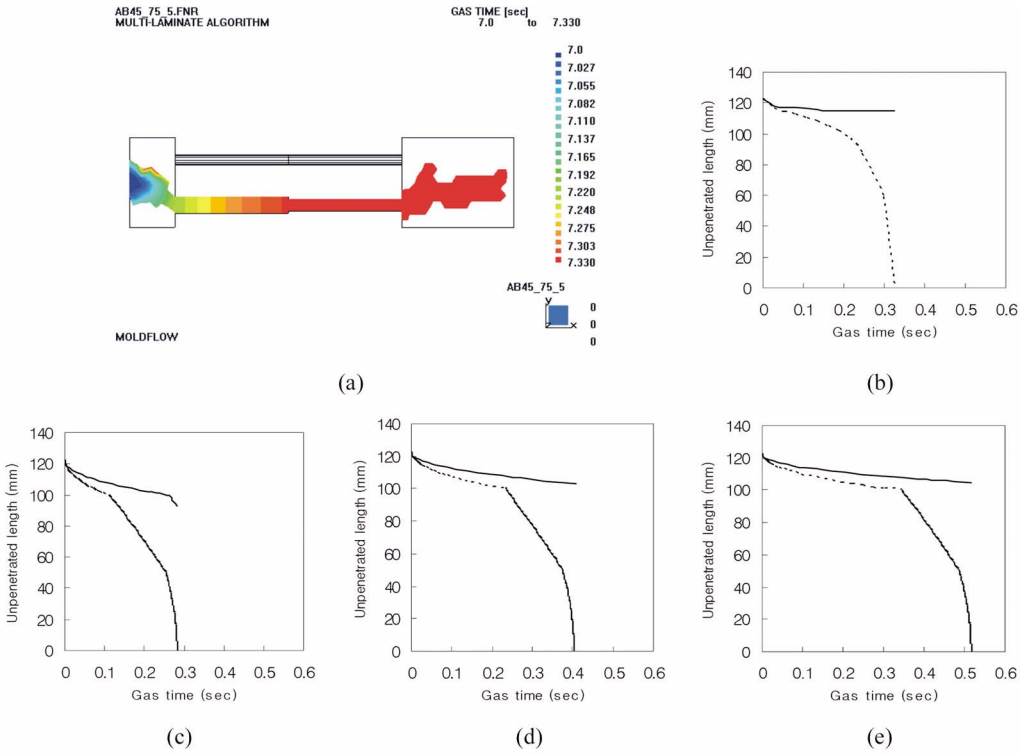

Fig. 10. (a) Pipe 11 with a diameter of 4.5 mm and a length of 50 mm is connected to pipe 12 with a diameter of 4.5 mm and a length of 50 mm. Pipe 21 with a diameter of 7.5 mm and a length of 50 mm is connected in series with pipe 22 with a diameter of 5 mm and a length of 50 mm; (b) Time evolution of gas penetration length from Fig. 10(a); Model predictions; (c) $\hat{\theta}$=0.93; (d) $\hat{\theta}$=2/3π; (e) $\hat{\theta}$=π (solid line: upper side, dotted line: lower side).

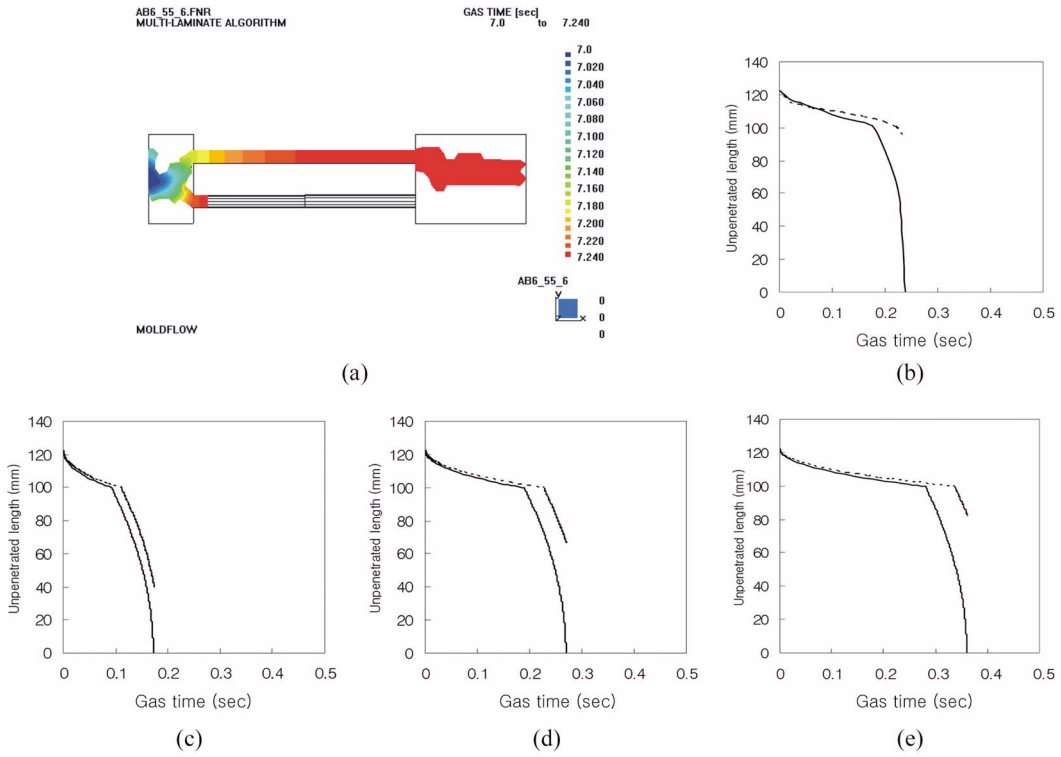

Fig. 11. (a) Pipe 11 with a diameter of 6 mm and a length of 50 mm is connected to pipe 12 with a diameter of 6 mm and a length of 50 mm. Pipe 21 with a diameter of 5.5 mm and a length of 50 mm is connected in series with pipe 22 with a diameter of 6 mm and a length of 50 mm; (b) Time evolution of gas penetration length from Fig. 11(a); Model predictions; (c) $\hat{\theta}$=0.93; (d) $\hat{\theta}$=2/3π; (e) $\hat{\theta}$=π (solid line: upper side, dotted line: lower side).

Table 5. Flow directions of simulation and developed flow model in Fig. 2

Case (a-b)	Simulation-results	Model-prediction (c)	Predicted gas-direction
Fig. 12(a)-(b)	U	Fig. 12(c)	U
Fig. 13(a)-(b)	U	Fig. 13(c)	U
Fig. 14(a)-(b)	U	Fig. 14(c)	U
Fig. 15(a)-(b)	U→L	Fig. 15(c)	U→L
Fig. 16(a)-(b)	U→L	Fig. 16(c)	U→L
Fig. 17(a)-(b)	L→U	Fig. 17(c)	L→U
Fig. 18(a)-(b)	L→U	Fig. 18(c)	L→U
Fig. 19(a)-(b)	L→U	Fig. 19(c)	L→U

*"U" and "L" denote "Upper" and "Lower", respectively.
*"U→L" denotes that gas flow is faster at the runner of upper side but its direction finally turns to lower side of the geometry.
*"L→U" denotes that gas flow is faster at the runner of lower side but its direction finally turns to upper side of the geometry.

predicted results were better when the value of $\hat{\theta}$ was applied as $2/3\pi$ radian than when the value of $\hat{\theta}$ was applied as 0.93 radian or π radian.

2. Situation when Cavities of Pipes and Runners are Involved in Configuration

Table 5 shows the predicted directions of gas flow of time-dependent developed flow model (Figs. 12(c) to 19(c)) as well as the results of simulation of Moldflow (Figs. 12(a)-(b) to 19(a)-(b)). Like Table 4, the predictions of developed flow model of Table 5 were also so quite consistent with the results of simulation that the proposed time-dependent flow model may be referred to describe very well the transient behavior of the movement of the interface of gas and melt-resin in the cavities. As in Table 5 the result of simulation of Figs. 15(a) and 16(a) (i.e., U→L) may be interpreted that the gas flow was slightly faster at the runner of the upper side and the direction of gas flow was finally reversed to the lower side of the geometry when the interface of gas and melt-resin was passing through the cavity of pipes. This is consistent with the results of part 1 of the paper where RT was slightly greater than unity while CRT was less than unity. On the other hand, as in Table 5, the result of simulation of Figs. 17(a) to 19(a) (i.e., L→U) may be interpreted as that the gas flow was slightly slower at the runner of the upper side and the direction of gas flow was finally reversed to the upper side of the geometry when the interface of gas and melt-resin was passing through the cavity of pipes. This is consistent with the results of part 1 of the paper where RT was slightly less than unity while CRT was greater than unity. Thus the effect of CRT was possibly expected so greater than that of RT, whose value is close to unity, in the result of simulation that the directiuon of gas flow would be finally changed to the other side of the cavity in the geometry. Note that CRT was advised, in part 1 of the paper, to be used as an adapted rule of thumb, especially when the value of RT is so close to unity. However, there

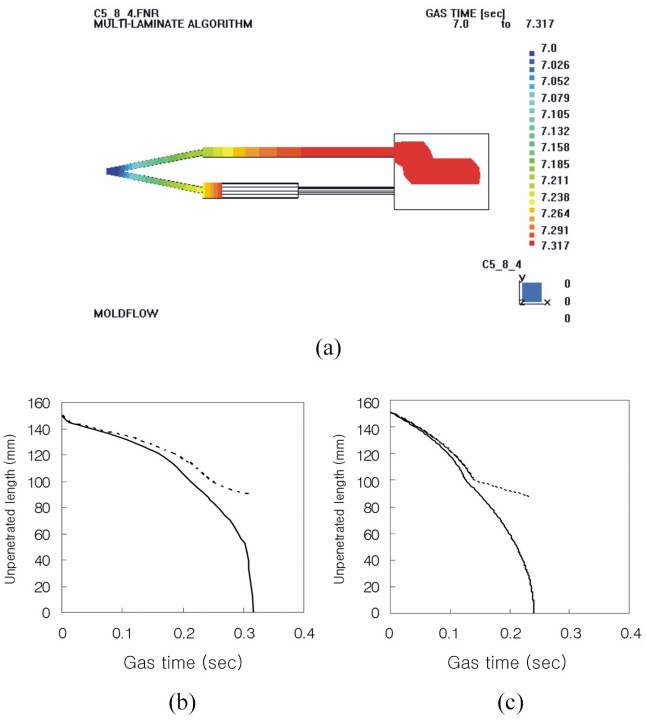

Fig. 12. (a) The geometry is similar to Fig. 4. Instead of a thick cavity of two square plates, branching runners with diameter of 3 mm are attached at the left hand side to deliver resin to pipes at both upper side and lower side; (b) Time evolution of gas penetration length from Fig. 12(a); (c) Model prediction (solid line: upper side, dotted line: lower side).

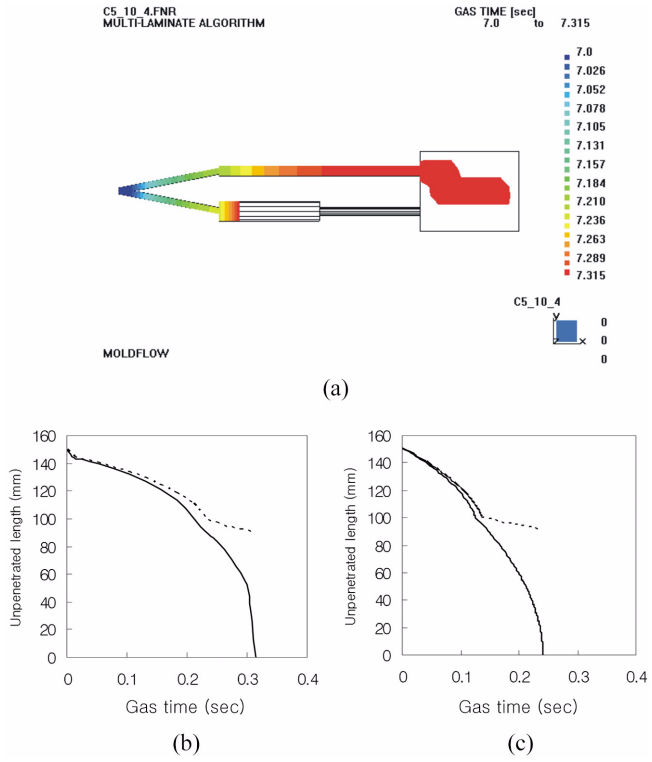

Fig. 13. (a) The geometry is similar to Fig. 5. Instead of a thick cavity of two square plates, branching runners with diameter of 3 mm are attached at the left hand side to deliver resin to pipes at both upper side and lower side; (b) Time evolution of gas penetration length from Fig. 13(a); (c) Model prediction (solid line: upper side, dotted line: lower side).

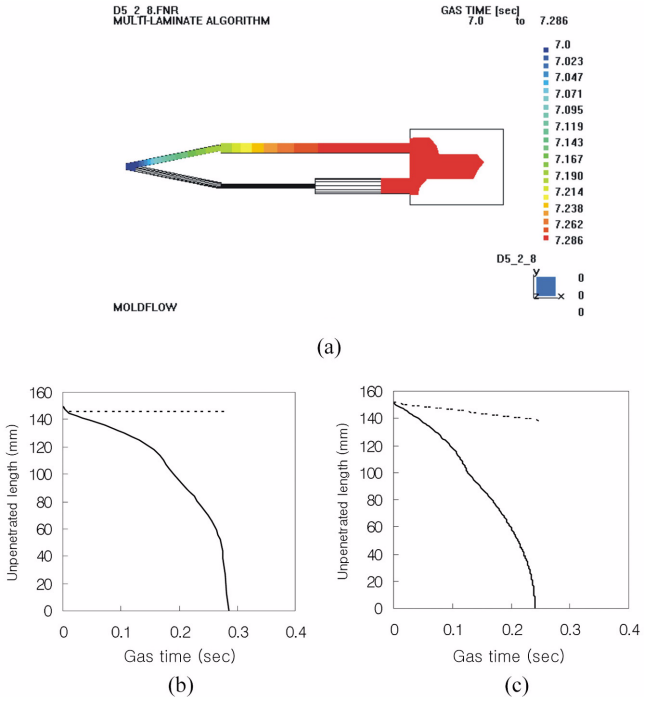

Fig. 14. (a) The geometry is similar to Fig. 6. Instead of a thick cavity of two square plates, branching runners with diameter of 3 mm are attached at the left hand side to deliver resin to pipes at both upper side and lower side; (b) Time evolution of gas penetration length from Fig. 14(a); (c) Model prediction (solid line: upper side, dotted line: lower side).

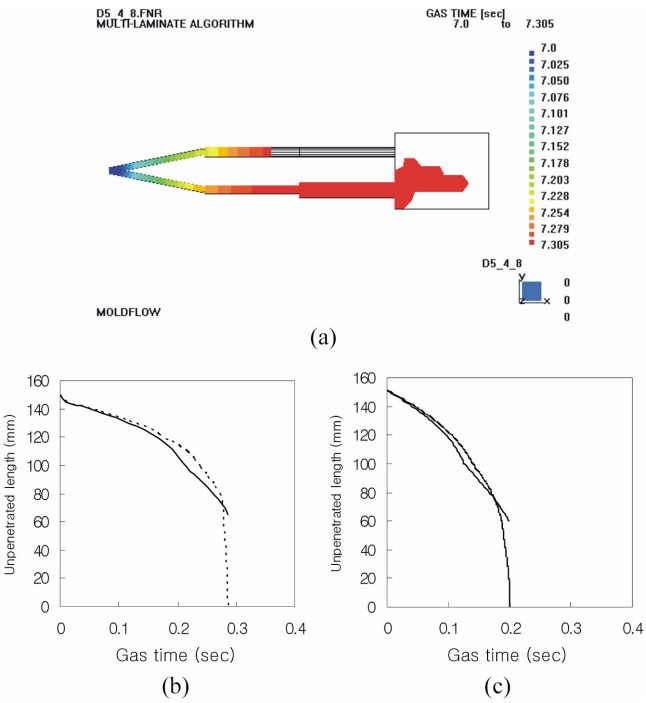

Fig. 15. (a) The geometry is similar to Fig. 7. Instead of a thick cavity of two square plates, branching runners with diameter of 3 mm are attached at the left hand side to deliver resin to pipes at both upper side and lower side; (b), Time evolution of gas penetration length from Fig. 15(a); (c) Model prediction (solid line: upper side, dotted line: lower side).

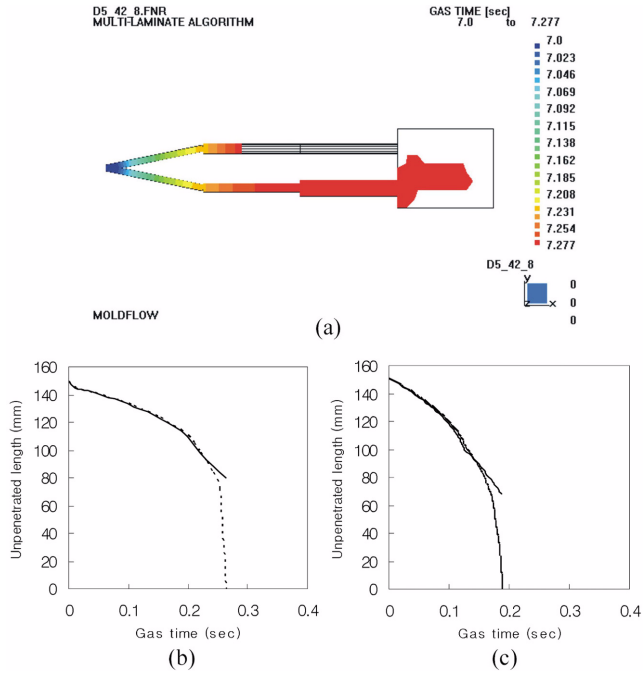

Fig. 16. (a) The geometry is similar to Fig. 7 except that diameter of pipe 21 is 4.2 mm. Instead of a thick cavity of two square plates, branching runners with diameter of 3 mm are attached at the left hand side to deliver resin to pipes at both upper side and lower side; (b), Time evolution of gas penetration length from Fig. 16(a); (c) Model prediction (solid line: upper side, dotted line: lower side)

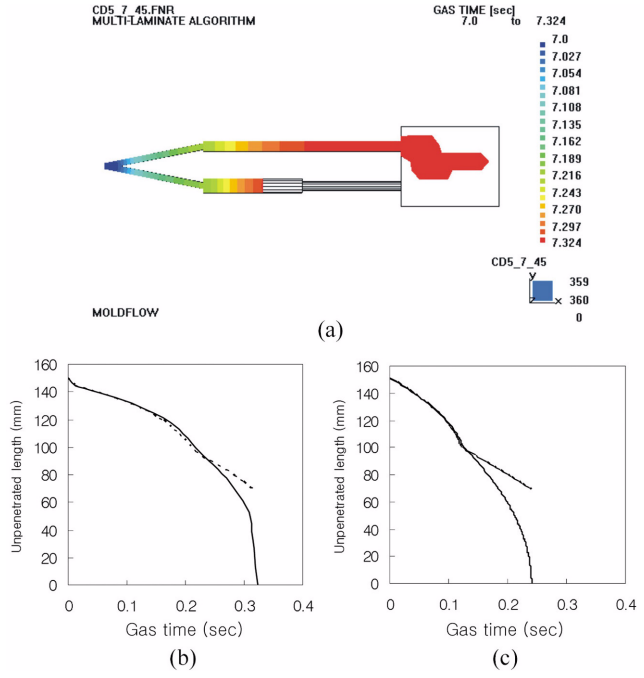

Fig. 17. (a) The geometry is similar to Fig. 8 except that diameter of pipe 21 is 7 mm. Instead of a thick cavity of two square plates, branching runners with diameter of 3 mm are attached at the left hand side to deliver resin to pipes at both upper side and lower side; (b) Time evolution of gas penetration length from Fig. 17(a); (c) Model prediction (solid line: upper side, dotted line: lower side).

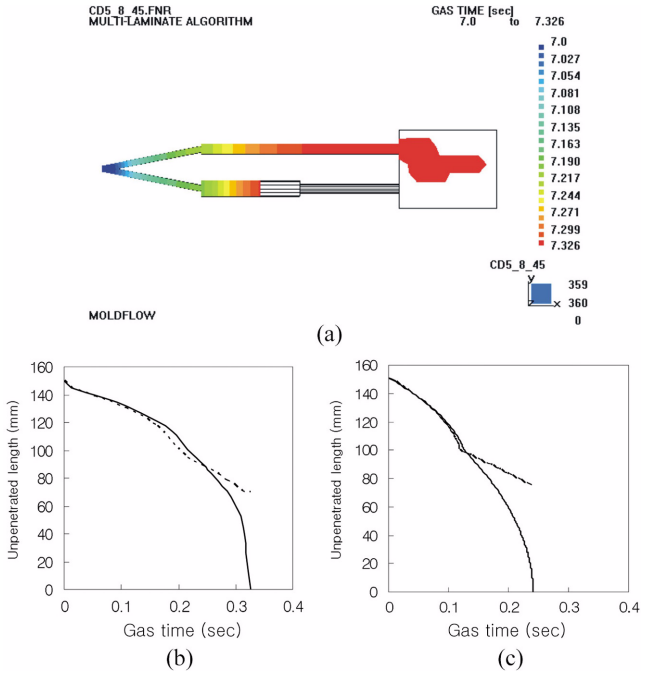

Fig. 18. (a) The geometry is similar to Fig. 8 except that diameter of pipe 21 is 8 mm. Instead of a thick cavity of two square plates, branching runners with diameter of 3 mm are attached at the left hand side to deliver resin to pipes at both upper side and lower side; (b) Time evolution of gas penetration length from Fig. 18(a); (c) Model prediction (solid line: upper side, dotted line: lower side).

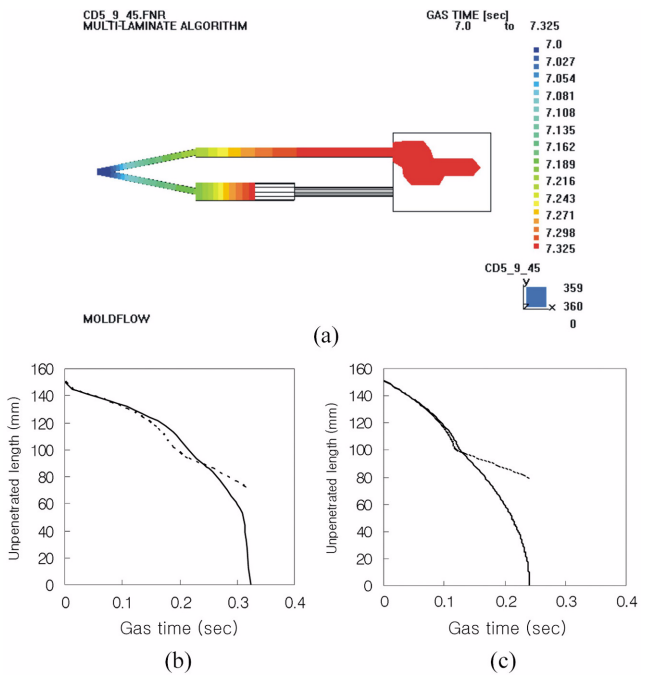

Fig. 19. (a) The geometry is similar to Fig. 8 except that diameter of pipe 21 is 9 mm. Instead of a thick cavity of two square plates, branching runners with diameter of 3 mm are attached at the left hand side to deliver resin to pipes at both upper side and lower side; (b) Time evolution of gas penetration length from Fig. 19(a); (c) Model prediction (solid line: upper side, dotted line: lower side)..

was no idea about which one finally prevails in the other case in part 1 of the paper, which may be treated successfully in the proposed developed model. It is amazing that the proposed developed model was able to predict exactly the cross-over between the trajectories of interface of upper and lower side as in Figs. 15(c) to 19(c), and it is also surprising to describe the time-dependent behavior so well, as in Figs. 12(c) to 19(c), that the result of the predictions by the developed model were quite consistent with the results of simulation by Moldflow.

CONCLUSION

Such a developed model as a time-dependent model was required to describe the transient behavior of the interface between gas phase and resin phase instead of a comparison of initial velocities in the upper side and lower side of the configuration, which was proposed and utilized to compare with the results of Moldflow in this 2nd part of the paper. The predictions of developed flow model were so consistent with the results of simulation that the proposed time-dependent flow model may be referred to describe very well the transient behavior of the movement of the interface of gas and melt-resin in the cavities.

In addition, the time-dependent model was also established and used to compare with the results of Moldflow when cavities of pipes and runners were involved in configuration. It is amazing that the proposed developed model was able to predict exactly the cross-over between the trajectories of interface of upper and lower side, and it is also surprising to describe the time dependent behavior so well that the result of the predictions by the developed model were quite consistent with the results of simulation by Moldflow. Thus the suggested time-dependent model may replace expensive commercial software to predict time-dependent behavior of the interface of gas and melt-resin which plays an important role for the design of gas channel and gas injection location in GAIM.

ACKNOWLEDGMENT

This research was supported (in part) by the Daegu University Research Grant, 2004.

NOMENCLATURE

D : diameter of pipe or conduit
D′ : diameter of a runner
h : distance between top or bottom plate and centerline of the cavity
H : distance between two parallel plates
L : length of pipe (filled with melt-resin) in the direction of flow
L(0) : initial length of pipe (filled with melt-resin) in the direction of flow
L′ : length of a runner (filled with melt-resin)
L′(0) : initial length of a runner (filled with melt-resin)
P : pressure
P_1 : pressure at $r=R_1$
P_0 : pressure at $r=R_0$
ΔP : pressure drop along the distance
Q : flow rate of melt resin

R_1 : radius of interface between gas and melt-resin
$R_1(0)$: radius of nozzle for melt resin- or gas-injection
R_0 : radius of initial polymer shut off
RT1 : ratio of initial resin radial velocities at $r=R_0/2$ of the cavity of two square flat plates connected to upper pipes and lower pipes as in Fig. 1.
RT2 : ratio of initial axial velocity of upper pipes and lower pipes without the cavity of two square flat plates
r : coordinate in cylindrical coordinate
t : time
V : average axial velocity
$\bar{v}_r$: average radial velocity at $r=R_0/2$
$\langle v_r \rangle$: average radial velocity

Greek Letters

ρ : density of polymer melt phase
$\hat{\theta}$: vertex angle of the fan-shaped radial flow
μ : Newtonian viscosity

Subscripts

1 : upper side
11 : the first pipe at upper side
12 : the second pipe at upper side
2 : lower side
21 : the first pipe at lower side
22 : the second pipe at lower side

REFERENCES

Lim, K. H., "Flow Direction when Fan Shaped Geometry is Applied in Gas Assisted Molding: 1. Theory of Flow Model and its Criterion to Predict Flow Directions," *Korean J. Chem. Eng.*, **21**, 48 (2004a).

Lim, K. H., "Gas Flow Direction under Heterogeneous Geometry Composed of a Pipe and a Cavity of Two Square-flat Plates in Gas Assisted Injection Molding," *Journal of Industrial and Engineering Chemistry*, **10**(3), 416 (2004b).

Lim, K. H., "Flow Directions in Gas Assisted Injection Molding when Cavities of Square Flat Plates and Pipes are Involved: 1. Theory of Flow Model and its Criterion," *Korean J. Chem. Eng.*, **21**, 1108 (2004c).

Lim, K. H. and Hong, S. H., "Flow Direction when Fan Shaped Geometry is Applied in Gas Assisted Molding: 2. Development of Flow Model and its Predictions," *Korean J. Chem. Eng.*, **21**, 59 (2004).

Lim, K. H. and Lee, E. J., "Predictions of Gas Flow Directions in Gas Assisted Injection Molding When Cavities and Runners are Involved," *Korean J. Chem. Eng.*, **20**, 592 (2003).

Lim, K. H. and Soh, Y. S., "The Diagnosis of Flow Direction under Fan Shaped Geometry in Gas Assisted Injection Molding," *Journal of Injection Molding Technology*, **3**, 31 (1999).

Soh, Y. S., "Control of Gas Direction in Gas Assisted Injection Molding," *Journal of Reinforced Plastics and Composites*, **19**, 955 (2000).

Soh, Y. S. and Lim, K. H., "Control of Gas Direction in Gas Assisted Injection Molding: Definition of Resistance to Velocity, $r_{\bar{V}}$," SPE ANTEC Tec. Papers, **60**, 482 (2002).